Optical detection of electron paramagnetic resonance in room-temperature electron-irradiated ZnO

L. S. Vlasenko* and G. D. Watkins
Department of Physics, Lehigh University, 16 Memorial Drive East, Bethlehem, Pennsylvania 18015-3182, USA
(Received 19 November 2004; published 21 March 2005)

The dominant defect observed in the photoluminescence (PL) of room-temperature electron-irradiated ZnO by optical detection of electron paramagnetic resonance (ODEPR) is determined to be the positively charged oxygen vacancy (V_O^+). Its spectrum, labeled L3, was previously observed in a 4.2 K *in situ* irradiation study [Yu. V. Gorelkinskii and G. D. Watkins, Phys. Rev. B **69**, 115212 (2004)], but it was thought there not to be stable at room temperature and was not identified. Here it is found to be stable to 400 °C, where it disappears. It is observed as a competing process (negative signal) to the dominant PL band produced by the irradiation at ~700 nm, but is positive in a weaker band at ~600 nm. Models are presented for its electrical level position in the gap to explain the results. Two other ODEPR signals are also detected, one of which is tentatively identified as also associated with the oxygen vacancy.

DOI: 10.1103/PhysRevB.71.125210 PACS number(s): 61.72.Ji, 61.82.Fk, 76.70.Hb, 78.55.Et

I. INTRODUCTION

There is currently growing interest in zinc oxide (ZnO) as a wide band gap semiconductor for possible electronic and optical applications. Readily grown as large single crystals, with a band gap of ~3.4 eV, it potentially offers many complementary and/or competitive advantages in these applications to the similar band gap material GaN, to which it provides, in addition, a close lattice match.[1]

Important to its successful device application is the understanding of its intrinsic defects, i.e., vacancies and interstitials, because they provide the various diffusion mechanisms involved in processing and device degradation, as well as often controlling, directly or indirectly, background doping, compensation, minority carrier lifetime, and luminescence efficiency. The only direct and unambiguous method for introducing simple vacancies and interstitials for experimental studies is by high energy electron irradiation, where single host atoms can be displaced from their lattice sites by recoil from an electron-nucleus Rutherford scattering event. In addition, the most successful experimental technique for identifying and studying the defects has often proven to be electron paramagnetic resonance, detected either directly (EPR) or optically (ODEPR). In the case of ZnO, early EPR studies in the 70's have already identified vacancies produced by electron irradiation on each of the two sublattices—V_{Zn}^- and V_{Zn}^0 on the Zn sublattice,[2–4] and V_O^+ on the O sublattice.[5,6] They were found to be stable at room temperature, but their stability at elevated temperatures was not explored.

Recently, our group has reported an ODEPR study in the photoluminescence (PL) of ZnO which was electron-irradiated *in situ* at 4.2 K.[7] In that preliminary study, changes in the UV-excited PL were observed to be produced by the irradiation and at several subsequent annealing stages up to room temperature. In addition, three ODEPR signals detected in the PL (PLODEPR), labeled L1, L2, and L3, were observed to emerge and disappear with the PL annealing stages. In these studies, the electron irradiation dosage was modest ($\sim 10^{16}$ e/cm^2), and after the room-temperature anneal, the ODEPR signals had disappeared and the PL had recovered approximately to its pre-irradiation state. The ODEPR signals were not identified, but because vacancies on the two sublattices had previously been established to be stable at room temperature, it was concluded that the various annealing stages below room temperature must be reflecting migration of interstitials on either one or both of the sublattices.

In the present study, we extend the PLODEPR studies to room-temperature electron-irradiatied ZnO samples to explore the vacancy- and interstitial-related defects that remain stable at that temperature, and their higher temperature annealing properties. One of our principal results is the discovery that the L3 signal, previously thought to disappear in a room-temperature anneal after 4.2 K electron irradiation,[7] is actually still present after room-temperature irradiation, and stable to 400 °C, where it disappears. It is identified here as arising from the positively charged oxygen vacancy (V_O^+), and tentative models for its electrical level structure in the gap will be discussed to explain the spectral dependence of excitation and luminescence associated with its observation. Two other ODEPR centers are also detected, one of which is tentatively identified also with the oxygen vacancy.

II. EXPERIMENTAL PROCEDURE

For the study, ZnO samples were cut from nominally undoped single crystal wafers obtained from several sources: (1) Eagle Picher, labeled EP, grown by seeded chemical vapor transport; (2) Cermet, labeled CE, advertised to be grown by a "patented melt process;" and (3) University Wafer Inc., labeled UW, for which the original growth method was unspecified. In addition, a sample cut from a single *c*-axis hexagonal crystallite grown from the vapor phase by Helbig at the Institute for Applied Physics, University of Erlangen, Germany, labeled HG, was also studied.

After a brief PL and PLODEPR characterization in the as-grown state, the samples were irradiated at room temperature with electrons from a 2.5 MeV van de Graaff accelera-

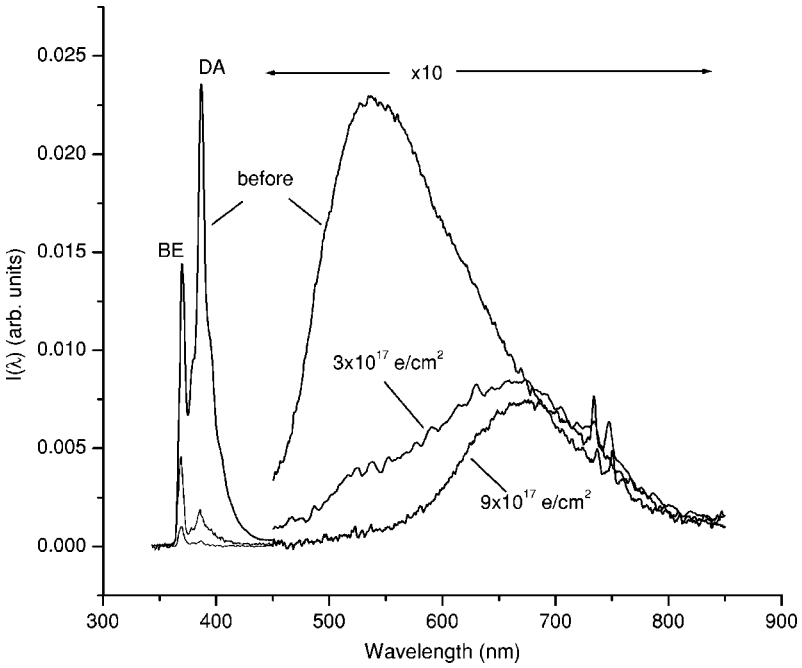

FIG. 1. PL under 351.1 nm excitation at $T = 1.7$ K of an EP ZnO sample vs 2.5 meV electron irradiation dose.

tor. For each, the irradiation proceeded in several stages up to a maximum dose of $\sim 9 \times 10^{17}$ e/cm^2, with PL and PLODEPR characterization at each stage. Isochronal anneals of one of the EP samples were subsequently performed under flowing nitrogen gas at atmospheric pressure.

The PL and PLODEPR were performed under excitation with the various ultraviolet (UV) and visible lines available from an Ar^+ ion laser (351.1, 363.8, 457.9, 476.5, 488, 496.5, 501.7, and 514.5 nm). The typical excitation power was ~20 mW. Detection of the luminescence was achieved in the visible and near UV by a silicon diode (EGG 250 UV) and in the near IR by a cooled Ge detector (North Coast EO817S), followed by lock-in detection synchronized to the frequency of a chopper in the excitation (for PL), or to the microwave on-off modulation frequency (for PLODEPR). All PL and PLODEPR studies were performed at pumped liquid He (~1.7 K) in a 35 GHz ODEPR spectrometer which has been described elsewhere.[8] The spectral dependence of the PL was determined by placing a 1/4 m Jarrell–Ash monochromator before the detector. For the ODEPR signals, the spectral dependence was determined in the visible region by placing a linearly variable interference filter (Oriel 7155) before the detector. In the near-IR region, selected fixed filters were used for the purpose. Where appropriate, the spectral dependences were corrected for the response of the detector, and in the case of the PL, by the response of the monochromator, as well. For determination of the ODEPR spectra g values, the value of $g_{\|}$ (1.9570) given by Carlos, Glaser, and Look[9] for the shallow effective mass donor signal, which was always present, was used as a magnetic field calibration correction.

III. RESULTS

In Fig. 1, we show the PL spectra for an EP sample under 351.1 nm excitation, before and after 2.5 MeV electron irradiation up to 9×10^{17} e/cm^2. As shown, a new broadband centered at ~700 nm grows in, while the neutral donor bound exciton, the distant donor-acceptor recombination (DA) bands, and an initially present broadband centered at ~540 cm are strongly suppressed. For the samples of different origin (CE, UW, HG), there were differences in the PL before irradiation, but the general result of electron irradiation was the same—production of the dominant 700 nm band, with a strong reduction in the pre-irradiation bands.

In Fig. 2, we show the ODEPR spectra observed in the Si

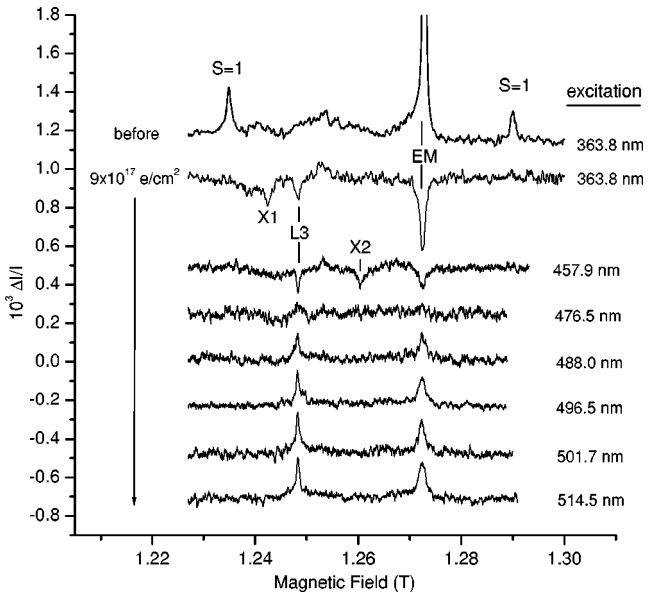

FIG. 2. ODEPR spectra, $\mathbf{B} \| c$ axis, observed in the spectral range 600–1100 nm for the EP sample of Fig. 1 before, and after, 9×10^{17} e/cm^2 irradiation with 2.5 MeV electrons. Before irradiation, ODEPR signals are observed only under UV excitation. After irradiation, visible excitation is also effective, with differences, as shown.

TABLE I. Spin Hamiltonian parameters.

Spectrum	$g_{\parallel}$	$g_{\perp}$
L3	1.9946(2)	1.9960(2)
V_O^+	1.9945(2)[a]	1.9960(2)[a]
EM	1.9570[b]	1.9552(2)
X1	2.0030(2)	~2.011
X2(V_O^+?)	1.9757(2)	1.9755(2)

[a]Reference 6.
[b]Taken as calibration marker from Ref. 9.

detector spectral range ($\lambda < 1100$ nm) for the PL of the EP sample of Fig. 1, before and after the final 9×10^{17} e/cm^2 irradiation. Before the irradiation, ODEPR spectra are seen only under UV excitation (351.1 or 363.8 nm) and consist, as shown, primarily of the effective mass shallow donor resonance (EM), and an $S=1$ center, both of which have been extensively studied by others previously.[9,10] After the irradiation, the $S=1$ signals have disappeared and three new signals have emerged. The g values for these signals are given in Table I, which immediately identifies one as L3, the signal previously reported to disappear upon annealing at room temperature after electron irradiation at cryogenic temperatures.[7] We tentatively label the other two X1 and X2. Shown also in the figure is the fact that visible excitation after the electron irradiation also produces the spectra, with important differences for different exciting wavelengths: X1 is seen only for UV excitation (351.1 and 363.8 nm), X2, only for 457.9 nm excitation, and L3 and EM together are seen throughout but change sign (become positive) for wavelengths beyond 476.5 nm.

In Fig. 3, we show, for the EP sample, the spectral dependence for (a) the PL, and (b) the ODEPR signals for two different excitations, 457.9 and 496.5 nm, which straddle the sign crossover region for L3 and EM shown in Fig. 2. It is clear from (a) that the dominant 700 nm band is not produced by 496.5 nm (or longer wavelength) excitation and, from (b), that the L3 (and EM, not shown) signals are positive in the PL at all wavelengths for the 496.5 nm (and longer wavelength) excitation, reflecting a broadband centered at ~600 nm for which the spin-dependent process involving L3 and EM is a *feeding* one. On the other hand, L3 (and EM, not shown) are negative in the strong 700 nm band excited by 457.9 nm (and shorter wavelengths) revealing the spin dependent L3/EM process as competing with it. X2 is seen only under the 457.9 nm excitation and reflects a competing process only with the 700 nm band. (No ODEPR signals appear to arise from the weak band seen in Fig. 3(a) at ~1030 nm. The band is real, disappearing after ~ one month at room temperature.)

Roughly similar results have been found for the CE, UW and HG samples in that, for each, the dominant signals after electron irradiation are X1, X2, L3, and EM. And the general spectral behavior of the three signals vs excitation and emission wavelength is similar to that of Figs. 2 and 3, although there are differences in their relative intensities. The main differences between the samples come in the ODEPR spectra before irradiation. For the CE and UW samples, the dominant ODEPR spectra before irradiation reveal DA pair recombination between the EM donor and the deep substitutional Li acceptor.[11] This suggests that the samples were probably grown by the hydrothermal method, for which LiOH is often a solvent.[12] For the HG sample, the dominant ODEPR signals involve vanadium, presumably an accidental

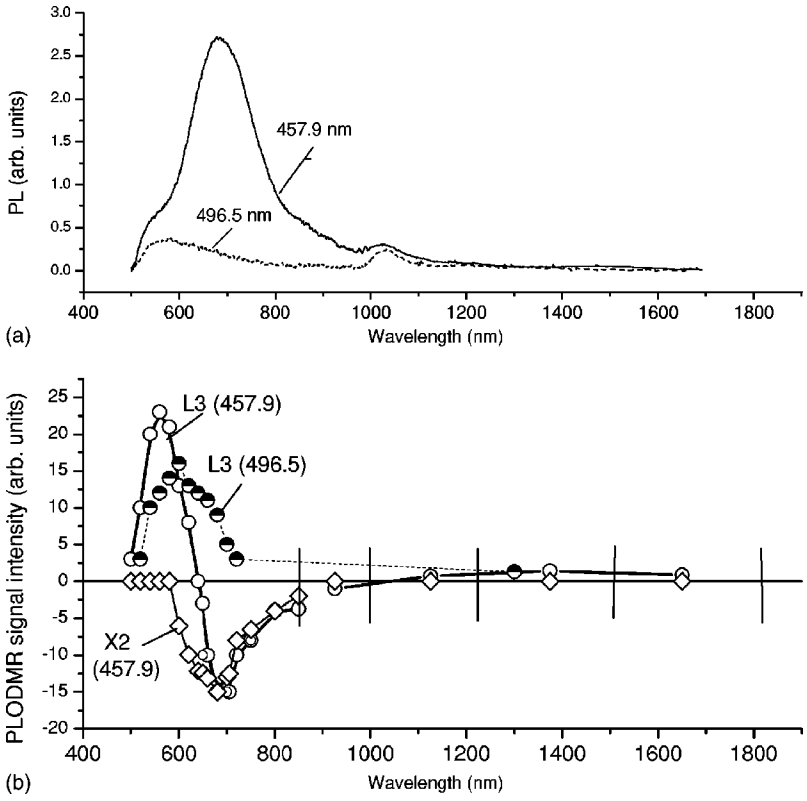

FIG. 3. Comparison of the spectral dependences of (a) the PL, and (b) the ODEPR signals, for excitation at two different wavelengths. The PL in (a) has been corrected for the monochromator response but neither (a) nor (b) has been corrected for detector response, which is common to both. Below 900 nm, the ODEPR spectral response was determined using the Oriel tunable interference filter with resolution ~20 nm. Above 900 nm the spectral width for each point (~150–300 nm) was limited by available high and low pass filters, and is indicated by vertical lines in (b).

impurity.[13] In each case, these signals decrease strongly in intensity as the electron irradiation proceeds, with X1, X2, and L3 ultimately dominating.

Isochronal annealing (30 min) of an EP sample which had been irradiated to a dose of 6×10^{17} e/cm^2 was performed in 100 °C steps, beginning at 100 °C. The ODEPR signals were monitored under each of the various excitation conditions of Fig. 2, and no change was observed until the 400 °C step, at which point X1, X2, and L3 disappeared together. A check of the PL at that point revealed the disappearance of the 700 nm band and substantial return of the pre-irradiation bands.

IV. DISCUSSION

A. L3(V_O^+)

In the earlier *in situ* 2.5 MeV electron irradiation studies at 4.2 K,[7] negative L3 and EM ODEPR signals were observed in a 700 nm PL band under UV excitation which emerged upon annealing at ~180 K. The PL band and the ODEPR signals were reported to disappear together after annealing at room temperature. For these studies, the irradiation dose was only 1.4×10^{16} e/cm^2. In the present studies, the dose was much greater, up to 9×10^{17} e/cm^2, and we find the 700 nm PL band still present at room temperature under UV excitation, along with the negative L3 and EM signals. We conclude therefore that although a substantial fraction of the defects giving rise to the 700 nm band apparently anneals at room temperature, some remain, and are stable to 400 °C, where our present study reveals them to finally disappear.

The values determined for L3 in Table I are clearly, within accuracy, equal to those of the single positively charged oxygen vacancy, V_O^+, which are also included in the table.[6] Now that we have determined that L3 is actually stable at room temperature, as had been previously established for V_O^+,[5,6] we can now conclude that L3 arises from V_O^+, and label it accordingly in our further discussion.

The identical sign and amplitude in Fig. 2 for the L3 and EM ODEPR signals versus various excitation wavelengths reveals clearly that the signals arise from the spin-dependent process

$$\mathrm{EM}^0 + V_O^+ \rightarrow \mathrm{EM}^+ + V_O^0, \qquad (1)$$

where an electron is transferred from a shallow effective mass donor to the positively charged oxygen vacancy. The signals are negative in the 700 nm band, revealing that the process is in competition with that involved in producing the 700 nm PL.

The EM and L3 signals are positive in a PL band centered ~600 nm, revealing that the transfer process of Eq. (1) is, in this case, positively involved in the production of the 600 nm band. Two possibilities suggest themselves: (a) Eq. (1) is the luminescence process itself. Extrapolating along the high energy side of the broad 600 nm band in Fig. 3(b) suggests the zero phonon line (ZPL) to be at ~500 nm (2.48 eV). With a low temperature band gap of 3.45 eV and a donor binding energy of ~50 meV, this requires the (0/+) single donor level of V_O to be deep in the band gap at $\sim E_V+0.9$ eV, as shown in Fig. 4(a). Alternatively, (b) the luminescence could result from subsequent hole capture by V_O^0. This would place the single donor level much higher in the gap at $\sim E_V+2.48$ eV, as shown in Fig. 4(b). In either case, the spin-dependent electron capture process of Eq. (1) could remain an essential part of the PL process.

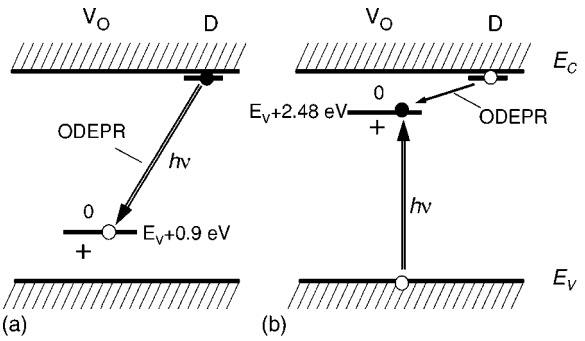

FIG. 4. Two possible models for the origin of the 600 nm PL band and the associated EM and V_O^+ ODEPR signals.

Theoretical estimates for the level positions of V_O have recently been made by two independent groups using local density approximation (LDA) techniques.[14,15] In both cases, negative-U ordering was predicted, with the (0/++) transition level high in the band gap at $\sim E_V+2.7$ eV. If correct, the V_O^+ charged state is thermodynamically unstable. But that is OK, since we are observing it during optical illumination in what would therefore be a metastable state. (Previous EPR studies of the defect apparently also required optical excitation for its observation.[5,6]) The results of one theory group estimated a negative-U value of 1.2 eV, which predicts the first donor level to be at $\sim E_V+2.1$ eV.[15] This is roughly consistent with the model in Fig. 4(b). The other group,[14] however, estimated a larger negative U, predicting the first donor level to be in the lower half of the band gap at $E_V+0.9$ eV, close to the requirement for the model in Fig. 4(a). The difference in the negative-U estimates appears to come from different ways of handling the band gap correction, which unfortunately is very large (the LDA band gap is only 0.9 eV, requiring corrections of up to ~2.5 eV). This necessary large band gap correction makes the accuracy of the predicted level positions difficult to assess. However, recognizing that a negative-U value as large as 1.2 eV is already surprisingly large, it could be argued that the results of Van de Walle[15] may be closer to reality, lending partial support to the model in Fig. 4(b).

Let us first, however, consider the model of Fig. 4(a) in more detail. Such a model is the usual first consideration in ODEPR studies, where Eq. (1) is the luminescence process itself. In such cases, the dominant excitation process is often found to be the direct optical ionization of the defect, i.e., the reverse reaction to Eq. (1) in which the electron is ionized to the conduction band and subsequently trapped at a shallow donor. A confirmation of that process would be a sharp cutoff in excitation efficiency when the excitation energy goes below that required for the ionization. However, from Fig. 2, it is clear that visible excitation is essentially uniformly efficient down to an energy of 2.41 eV (514.5 nm), inconsistent

with the required ionization energy of 2.54 eV, particularly when a ~0.4 eV Stokes shift is added (difference between the 600 nm PL maximum and the estimated 500 nm ZPL). This observation strongly suggests that the primary excitation process is the production of electrons and holes, which in their sequential capture and recombination at the defect produce the PL. The visible excitation energies are well below the band gap energy $E_G = 3.45$ eV required for direct production of electrons and holes. However, because of the many deep level defects undoubtedly present as a result of the electron irradiation, efficient mechanisms do, of course, exist for the production of both holes and electrons by optical excitation energies well below E_G.

The evidence that electron-hole recombination is involved in the PL does not rule out the model of Fig. 4(a). However, it does make possible the model of Fig. 4(b), which requires it. In Fig. 4(b), the luminescence results from the nonspin-dependent capture of holes, with the ODEPR arising from the electron capture process still required now in the PL cycle. This, plus the better agreement with the theoretical estimate of the $(0/+)$ V_O single donor level position, suggests that Fig. 4(b) may be the correct model.

In Fig. 3, positive EM and L3 signals are also observed weakly in a long tail of the PL into the infrared. In either model of Fig. 4, this could reflect the other half of the pumping cycle—in (a), the hole capture; in (b), the spin-dependent electron capture.

B. X2(V_O?)

In Table I, note that the g values of X2 are accurately given by the average of the g values for EM and L3. This interesting coincidence is precisely the result expected for close EM/L3 pairs for which the exchange interaction in the excited state is sufficiently larger than $(g_{L3}-g_{EM})\mu_B B$, the Zeeman energy difference between the two centers, to produce a triplet $S=1$ system. With the extended orbit of an overlapping shallow EM center, the angular dependence of the dipole-dipole interaction between the spins on the two centers might not be sufficiently strong to produce significant broadening due to a distribution of fine structure D terms. The fact that it is excited by 457.9 nm (2.71 eV) and not by 476 nm (2.60 eV) or longer wavelengths could be interpreted as the onset of direct excitation for close pairs, as in the model of Fig. 4(a). Here, the excitation ZPL should be close to the estimated value for the ZPL of the PL at ~2.48 eV, because no Coulomb interaction exists in either ground or excited state of Eq. (1). Adding a fraction of the estimated ~0.3 eV Stokes shift makes this interpretation at least consistent with the level positions in Fig. 4(a). The fact that UV excitation does not produce X2 could reflect the relatively low fractional concentration of the sufficiently close pairs and the resultant requirement of bulk optical penetration, as provided by light sufficiently lower than the band gap energy.

An alternative interpretation is that it arises from V_O^+, with a shallow effective mass electron bound Coulombically to it, no nearby donor required. As such it is a triplet exciton bound to V_O^0. The arguments above for the ODEPR character and the excitation properties remain essentially the same. Either interpretation is best explained by the model of Fig. 4(a).

However, although it shows up as a negative signal in the 700 nm band, it does not appear to show up as a measurable positive signal in the 600 nm band. This is less easy to understand in terms of either of the models in Fig. 4.

C. X1

The line is narrow with $B \| c$ axis, as shown in Fig. 2, but it broadens and shifts to lower field as the crystal is rotated away. It can be followed reliably only for ~40°, so the estimate for $g_\perp$ in Table I is only approximate, as indicated. We have no interpretation of the defect giving rise to X1. Since it is observed only under UV excitation the defect may exist only near the sample surface. Alternatively, it may, of course, be a bulk defect but require band to band excitation either for its direct excitation or for sufficient bulk electron-hole pair production for recombination through it to be significant. Until more experimental information is available for it, we will not consider it further.

D. 700 nm band

The 700 nm band is the dominant feature in the PL produced by the room-temperature electron irradiation. Coupled with information from earlier studies,[7] we know that after a 4.2 K irradiation, the band emerges only after anneal at ~180 K and that a substantial fraction, but not all, of it disappears in anneal at room temperature. The remaining part, studied here, is stable to 400 °C. It is clearly important, arising from some process involving the intrinsic defects produced by the electron irradiation. The fact that it emerges at ~180 K reveals, in addition, that rearrangement and/or migration of one of the primary defects must be involved to produce it. Since it has been established that vacancies on the two sublattices are stable at room temperature,[2–6] the migrating species must be one of the two interstitials. Beyond that, we know nothing concrete, because no positive ODEPR signals have been observed in it to reveal properties of the defect directly involved in its production.

V. SUMMARY

The dominant defect observed by ODEPR in ZnO irradiated by 2.5 MeV electrons at room temperature is identified as the oxygen vacancy in its singly positive charge state V_O^+. The spin-dependent process giving rise to its ODEPR signal, labeled L3, is the transfer of an electron from a shallow effective mass donor EM^0 to V_O^+, as given in Eq. (1). It is observed both as a competing process in the dominant 700 nm band produced by the irradiation, and as a feeding process in a weaker 600 nm band. Two possible models have been proposed to explain its role in the 600 nm PL production, one, in Fig. 4(a), placing its single donor level at ~0.9 eV above the valence band edge, the other, in Fig. 4(b), in the upper half of the band gap at $\sim E_V + 2.48$ eV. The first agrees closely with the theoretical estimate of Zhang, Wei, and Zunger[14] the second with the estimate of Van de Walle.[15]

An additional ODEPR signal, labeled X2, is tentatively identified as also involving the oxygen vacancy. It could arise either from an exciton bound to isolated V_O^0, or a close exchange-coupled EM^0-V_O^+ pair, the resulting ODEPR signal being essentially the same for either. If the identification is correct, its behavior under optical excitation would best be understood in terms of the model of Fig. 4(a), with the vacancy donor level at $\sim E_V+0.9$ eV. On the other hand, we have argued that the large negative-U estimate by Zhang, Wei, and Zunger, which is necessary to lower the oxygen vacancy donor level to that value, may be unrealistic. As a result, a selection between the two models cannot be made at this stage, and will have to wait either for additional experiments, or critical resolution of the different theoretical results.

The origin of the dominant 700 nm band produced by the electron irradiation remains unknown. Its appearance at $\sim$180 K after 4.2 K electron irradiation reveals that migration of one or the other of the interstitials on the two sublattices must be involved in its origin at that temperature. Its partial anneal at room temperature also suggests the same at that temperature. However, no positive ODEPR signals are observed in it to reveal its defect identity, and that important part of the story must remain for future studies.

ACKNOWLEDGMENTS

We thank G. Cantwell, Michael Stavola, Steve Pearton, and Joerg Weber for supplying the various ZnO samples used in the study. The research was supported by the National Science Foundation, Grant No. DMR-00-93784.

*Present address: A. F. Ioffe Physico-Technical Institute, Russian Academy of Sciences, 194021, St. Petersburg, Russia.

[1] See the recent review by D. C. Look, Mater. Sci. Eng., B **80**, 383 (2001).
[2] A. L. Taylor, G. Filipovich, and G. K. Lindeberg, Solid State Commun. **8**, 1359 (1970).
[3] D. Galland and A. Hervé, Phys. Lett. **33A**, 1 (1970).
[4] D. Galland and A. Hervé, Solid State Commun. **14**, 953 (1974).
[5] J. M. Smith and V. H. Vehse, Phys. Lett. **31A**, 147 (1970).
[6] C. Gonzales, D. Galland, and A. Hervé, Phys. Status Solidi B **72**, 309 (1975).
[7] Yu. V. Gorelkinskii and G. D. Watkins, Phys. Rev. B **69**, 115212 (2004).
[8] M. H. Nazaré, P. W. Mason, G. D. Watkins, and H. Kanda, Phys. Rev. B **51**, 16 741 (1995).
[9] W. E. Carlos, E. R. Glaser, and D. C. Look, Physica B **308–310**, 976 (2001).
[10] F. Leiter, H. Zhou, F. Henecker, A. Hofstaetter, D. M. Hofmann, and B. K. Meyer, Physica B **308–310**, 908 (2001).
[11] R. T. Cox, D. Block, A. Hervé, R. Picard, C. Santier, and R. Helbig, Solid State Commun. **25**, 77 (1978).
[12] T. Sekiguchi, S. Miyashita, K. Obara, T. Shishido, and N. Sakagumi, J. Cryst. Growth **214/215**, 72 (2000).
[13] L. S. Vlasenko and G. D. Watkins, Phys. Rev. B **71**, 115205 (2005).
[14] S. B. Zhang, S.-H. Wei, and A. Zunger, Phys. Rev. B **63**, 075205 (2001).
[15] C. G. Van de Walle, Physica B **308–310**, 899 (2001).